Innovative Use of Membrane Contactor as Condenser for Heat Recovery in Carbon Capture

ARTICLE *in* ENVIRONMENTAL SCIENCE AND TECHNOLOGY · JANUARY 2015

Impact Factor: 5.33 · DOI: 10.1021/es504526s · Source: PubMed

4 AUTHORS, INCLUDING:

Shuaifei Zhao
The Commonwealth Scientific and Industrial …
17 PUBLICATIONS **611** CITATIONS
SEE PROFILE

P. H. M. Feron
The Commonwealth Scientific and Industrial …
117 PUBLICATIONS **2,595** CITATIONS
SEE PROFILE

Environmental Science & Technology

Article

pubs.acs.org/est

Innovative Use of Membrane Contactor as Condenser for Heat Recovery in Carbon Capture

Shuiping Yan,[†,‡] Shuaifei Zhao,[*,†] Leigh Wardhaugh,[†] and Paul H. M. Feron[†]

[†]CSIRO Energy Technology, Post Office Box 330, Newcastle, New South Wales 2300, Australia

[‡]College of Engineering, Huazhong Agricultural University, Wuhan 430070, People's Republic of China

Supporting Information

ABSTRACT: The gas−liquid membrane contactor generally used as a nonselective gas absorption enhancement device is innovatively proposed as a condenser for heat recovery in liquid-absorbent-based carbon capture. The membrane condenser is used as a heat exchanger to recover the latent heat of the exiting vapor from the desorber, and it can help achieve significant energy savings when proper membranes with high heat-transfer coefficients are used. Theoretical thermodynamic analysis of mass and heat transfer in the membrane condensation system shows that heat recovery increases dramatically as inlet gas temperature rises and outlet gas temperature falls. The optimal split mass flow rate is determined by the inlet gas temperature and the overall heat-transfer coefficient in the condensation system. The required membrane area is also strongly dependent on the overall heat-transfer coefficient, particularly at higher inlet gas temperatures. Mass transfer across the membrane has an insignificant effect on heat transfer and heat recovery, suggesting that membrane wetting may not be an issue when a membrane condenser is used for heat recovery. Our analysis provides important insights into the energy recovery performance of the membrane condensation system as well as selection of operational parameters, such as split mass flow rate and membrane area, thickness, and thermal conductivity.

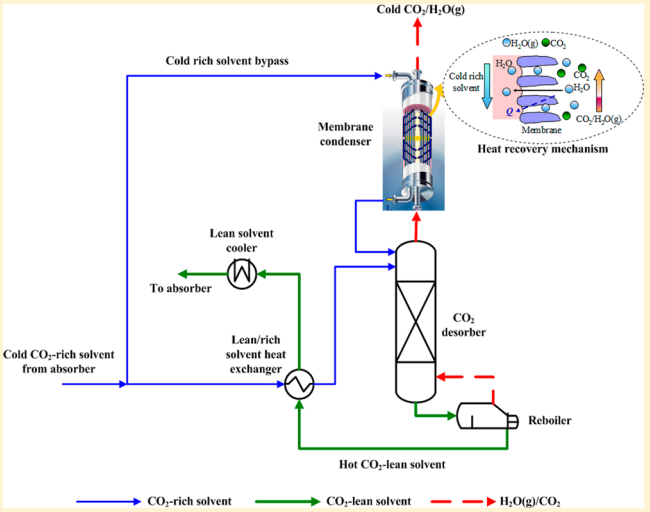

1. INTRODUCTION

CO_2 capture and storage (or sequestration), CCS, is recognized as one of the most important strategies to combat human-induced climate change.[1−3] In the CCS chain, the separation stage (i.e., CO_2 capture) is energy-intensive, accounting for around 70% of the total costs.[4] Generally carbon capture can be performed by three ways: postcombustion carbon capture, precombustion carbon capture, and oxyfuel combustion. Among them, postcombustion carbon capture (PCC) has the greatest potential for large-scale implementation in the near future, because it can be retrofitted to existing units in power plants.

Various technologies have been intensively investigated for carbon capture, such as liquid chemical absorption,[2,5] solid adsorption,[6] and membrane separation.[1,7−9] However, state-of-the-art capture technology is still based on a liquid absorbent that chemically reacts with CO_2.[10,11] Since 2007, the Commonwealth Scientific and Industrial Research Organisation (CSIRO) has worked with power companies to establish three absorbent-based PCC pilot plants around Australia, with capture capacities ranging from 100 to 500 kg of $CO_2 \cdot h^{-1}$.[12] We have gained considerable knowledge and experience from these plants in terms of energy performance,[11,13] process modification,[14−16] and absorbent development and validation.[17,18]

A typical process configuration for liquid-absorbent-based PCC can be seen in Figure S1 in Supporting Information. Flue gas from the power station passes through a pretreatment column, an absorbing column (i.e., absorber), and a stripping column (i.e., desorber or stripper). The energy required for regenerating the liquid absorbent in the stripping column is extracted from the steam produced by the power station. This steam is therefore not available for power generation, significantly reducing the power station's output. Typical output (i.e., plant power) reductions for 90% capture of CO_2 are around 30%. It is therefore necessary to improve the absorbent regeneration process by minimizing the thermal energy requirement in the desorber.

The starting point is to analyze the thermal energy requirement in more detail. In the stripping column, a huge amount of thermal energy is required for (i) bringing the liquid

Received: September 16, 2014
Revised: December 12, 2014
Accepted: January 15, 2015
Published: January 15, 2015

DOI: 10.1021/es504526s
Environ. Sci. Technol. 2015, 49, 2532−2540

absorbent up to the regeneration temperature, which is a function of the CO_2 loading of the absorbent; (ii) breaking the bond between CO_2 and the active component in the absorbent, which is determined by the chemical formulation of the liquid absorbent; and (iii) solvent evaporation in which water vapor (or steam) leaves the stripper together with the CO_2, which is determined by the temperature of the water-vapor-saturated CO_2 stream. The overall energy penalty also incorporates electricity use in the capture and compression process. The total penalty is, however, to a large extent determined by the thermal energy required to release CO_2 from the liquid absorbent, typically ~4 MJ·(kg of CO_2)$^{-1}$ for monoethanolamine (MEA).[19] Depending on the fuel type, this represents between 20% and 40% of the energy contained in the incoming fuel.

The ongoing development of new liquid absorbents will very likely reduce the first two contributions; that is, new amines with lower binding energy and higher CO_2 loadings have been identified.[18] However, the energy required for the production of stripping steam is still needed. All the energy needed for regeneration is brought in via the stripping steam and is transferred to the liquid absorbent via condensation. Hence, efficient control of the steam balance is extremely important for energy performance of the capture process.

In a typical PCC process, the water-vapor-saturated CO_2 stream from the desorber contains a large amount of heat at high temperature, which is transferred to the cooling water via a condenser (Figure S1, Supporting Information). To reduce heat loss due to vapor evaporation in the stripper, several process modifications have been investigated, such as vapor recompression and rich split.[14,15,20] In the rich split modification, a conventional heat exchanger was studied, and rate-based modeling showed that energy reductions were 6% for MEA and 10% for piperazine (PZ).[20]

In this study, we propose a novel membrane-assisted liquid absorbent regeneration (MALAR) process by employing a gas−liquid membrane contactor as the condenser to recover the evaporation heat, aiming to reduce the thermal energy requirement of carbon capture.[21,22] This is an innovative use of a membrane contactor compared with their conventional use as nonselective barriers for absorption enhancement in carbon capture.[23−25] Using a membrane contactor as the novel heat exchanger provides the following advantages over a conventional heat exchanger: (1) A membrane heat exchanger may perform better in heat recovery since both mass transfer and heat transfer can occur, whereas only heat transfer occurs in a conventional heat exchanger. (2) Conventional heat exchangers are generally used for (or are more efficient in) high-grade (i.e., high-temperature) heat recovery. Therefore, they have certain temperature requirements and material constraints. A membrane condenser can overcome these drawbacks. (3) A membrane contactor has an extremely high interfacial area, offering great benefits in process intensification due to its compactness.[26−29] To achieve these benefits, membrane materials with desirable properties should be carefully selected and experimentally verified for use in a membrane contactor/condenser. However, such work is beyond the scope of this study. Instead, this work aims to provide a broad view of energy recovery performance and the selection of operational parameters (e.g., split mass flow rate and membrane area), which are dependent on the membrane properties.

Thermodynamic analysis of mass and heat transfer in the membrane condensation system is carried out in the present study. The energy-saving potential of the membrane condensation system is estimated. The split mass flow rate, required membrane area, outlet solvent temperature, and their correlations are determined by solving the mass- and heat-transfer equations in the membrane condenser. Three scenarios (zero mass transfer, complete mass transfer, and partial mass transfer across the membrane) are considered in the analysis. Our analysis provides important insights into the energy recovery performance of the membrane condensation system as well as the selection of operational parameters.

2. THEORETICAL DEVELOPMENT

2.1. Novel Membrane Condensation System Incorporated into Liquid Absorbent Regeneration in Post-combustion Carbon Capture. A schematic diagram of the membrane condensation system incorporated into liquid absorbent regeneration is presented in Figure 1. After a solvent

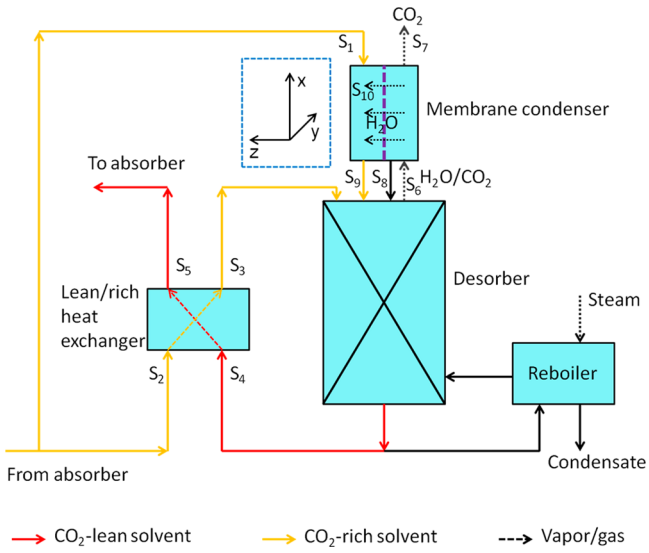

Figure 1. Schematic diagram of the membrane condensation system incorporated into liquid absorbent regeneration.

absorbs CO_2 from the flue gas, it becomes a CO_2-rich absorbent and can be split into two streams, S_1 and S_2. S_1 flows to a membrane condenser and S_2 flows to the lean/rich heat exchanger. After heat exchange with the flow (S_4) from the desorber, S_2 is warmed up to S_3, going to the desorber; and S_4 is cooled down to S_5, flowing to the absorber. On top of the desorber, the steam (i.e., water vapor) saturated CO_2 stream (S_6) goes to a membrane condenser. After membrane condensation, partial water vapor (S_{10}), with its associated latent heat, can be recovered by the relatively cold stream (S_1). The partial water vapor is condensed (S_8), flowing back to the desorber. Simultaneously, S_1 warms up to S_9 and S_6 cools down to S_7. S_1−S_{10} represent the liquid or gas streams, and their corresponding temperatures and mass flow rates are denoted as t_1−t_{10} and m_1−m_{10}, respectively.

Note that (i) trace organic solvent vapor loss is ignored in the process and (ii) the process can be applied to general liquid-absorbent-based CO_2 absorption−desorption processes without consideration of the absorbent type. According to the operation of our Tarong PCC pilot plant in Queensland,[30] typical values for the temperatures (t_1−t_{10}) and mass flow rates (m_1−m_{10}) are shown in Table 1.

DOI: 10.1021/es504526s
Environ. Sci. Technol. 2015, 49, 2532−2540

Table 1. Approximate Temperatures and Mass Flow Rates in Post-Combustion Carbon Capture[a]

temperature (°C)		mass flow rate[b] (kg·h^{-1})	
t_1	45	m_1	varying
t_2	45	m_2	varying
t_3	100	m_3	$= m_2$
t_4	115	m_4	1900
t_5	70	m_5	1900
t_6	90	m_6	90
t_7	*c*	m_7	70
t_8	*c*	m_8	*c*
t_9	*c*	m_9	*c*
t_{10}	*c*	m_{10}	*c*

[a]Data are based on our Tarong pilot plant in Queensland with 30 wt % MEA as the absorbent. [b]$m_1 + m_2 \approx 2000$ kg·h^{-1}. [c]To be evaluated.

The following theoretical analysis is based on several assumptions that are close to practical conditions: (i) The membrane condenser and the lean/rich heat exchanger are perfect thermally insulated systems (i.e., without any external heat loss). (ii) System pressure in the desorber and membrane condenser is 1.8 bar. (iii) Fluids along the membrane condenser are under countercurrent flow. (iv) Monoethanolamine (MEA, 30 wt %) solution is selected as the model absorbent, and the heat capacities of rich and lean solvents are constant in the temperature change range (3.4 and 3.5 kJ·kg^{-1}·K^{-1}, respectively).[31−33] (v) The membrane within the condensation system is perfectly CO_2-resistant (i.e., without any CO_2 transfer across the membrane).

Theoretically, CO_2 is less likely to transfer across the membrane from the gas side into the rich solvent side since the solvent has been loaded with CO_2. Even if a small amount of CO_2 transfers across the membrane, it will have an insignificant effect on the process performance of the condensation system. Three scenarios are considered in the following analysis: limited mass (i.e., water vapor) transfer, complete mass transfer, and partial mass transfer across the membrane.

2.2. Scenario 1: Limited Mass Transfer across Membrane into Absorbent. In this scenario, almost all the water vapor condenses on the membrane surface on the gas side and goes back to the desorber. The vapor transfer across the membrane is negligible (i.e., $m_{10} = 0$), whereas the latent heat via membrane condensation and conduction can still be transferred into the absorbent. Scenario 1 could occur when a wetted porous membrane or a dense membrane is used in the condensation system, allowing the membrane condenser to be regarded as a heat exchanger. Heat transfer (Q_m) across the membrane (direction *z* in Figure 1), which is constant at steady state, can be expressed by

$$Q_m = H_m(T_h - T_c)\frac{A}{L}\,dx = \lambda_m \frac{dT(z)}{dz}\frac{A}{L}\,dx \tag{1}$$

where *T* is temperature (kelvins) and the subscripts m, h, and c refer to membrane, hot gas stream, and cold liquid flow, respectively. *A* is the membrane area (square meters), *L* is the membrane module length (meters), H_m is the heat-transfer coefficient of the membrane (watts per square meter per kelvin), and λ_m is the thermal conductivity of the membrane (in the range 0.04−0.06 W·m^{-1}·K^{-1} for polymeric membranes).[34] The correlation between H_m and λ_m is given by

$$H_m = \frac{\lambda_m}{\delta_m} \tag{2}$$

where δ_m is the membrane thickness (meters) and

$$\lambda_m = \varepsilon\lambda_{air} + (1 - \varepsilon)\lambda_{solid} \tag{3}$$

where ε is the membrane porosity and λ_{air} and λ_{solid} are the thermal conductivities of air trapped in the pores and solid membrane material, respectively. The thermal conductivity of air (~0.027 W·m^{-1}·K^{-1} at 40 °C) is 1 order of magnitude lower than that of solid membrane material (~0.2 W·m^{-1}·K^{-1}).[35] Therefore, heat-transfer efficiency via membrane conduction can be improved by selecting a membrane with low porosity.

The heat obtained on the cold absorbent side (Q_c) can be expressed by

$$\begin{aligned} Q_c &= m_1(h_{c,o} - h_{c,i}) \\ &= m_1 c_{p,c}(T_{c,o} - T_{c,i}) \\ &= m_1 \int_{T_i}^{T_9} c_{p,c}\,dT \end{aligned} \tag{4}$$

where *h* is the specific enthalpy of the fluid (kilojoules per kilogram); subscripts o and i represent outlet and inlet, respectively; and c_p is the specific heat capacity (kilojoules per kilogram per kelvin), which can be assumed to be a constant.

After membrane surface condensation, the heat back to the desorber (Q_8) can be written as

$$Q_8 = m_8 h_w(T_{h,i}) \tag{5}$$

where $h_w(T_{h,i})$ is the specific enthalpy of the condensed water at the inlet gas stream temperature ($T_{h,i}$).

As the membrane condenser is a perfect thermally insulated and CO_2-resistant system, the total heat recovery (Q_r) can be written as

$$Q_r = m_{6,H_2O}h_{6,H_2O} - m_{7,H_2O}h_{7,H_2O} + (h_{6,CO_2} - h_{7,CO_2})\, m_{CO_2} \tag{6}$$

In this scenario, the heat balance can be expressed by

$$Q_m = Q_c \tag{7}$$

$$Q_c + Q_8 = Q_r \tag{8}$$

2.3. Scenario 2: Complete Mass Transfer through Membrane into Absorbent. In this scenario, all the water vapor in the gas stream (S_6) transfers and then condenses into the cold absorbent; that is, there is no vapor condensation on the gas side ($m_8 = 0$). Heat transfer occurs in association with mass transfer through the membrane.

2.3.1. Mass Transfer in Membrane Condenser. If $m_8 = 0$ (Figure 2), it is easy to obtain the transmembrane mass balance:

$$m_{10} = m_6 - m_7 = m_9 - m_1 \tag{9}$$

where m_{10} is the mass flow rate across the membrane.

For each differential segment of the membrane module, the mass balance can be described as

$$\frac{dm_h(x)}{dx} = \frac{dm_c(x)}{dx} = \frac{A}{L}J_m(x) \tag{10}$$

where $m_h(x)$ and $m_c(x)$ are the mass flow rates (kilograms per hour) of hot gas and cold solvent at axial position *x* in the

DOI: 10.1021/es504526s
Environ. Sci. Technol. 2015, 49, 2532−2540

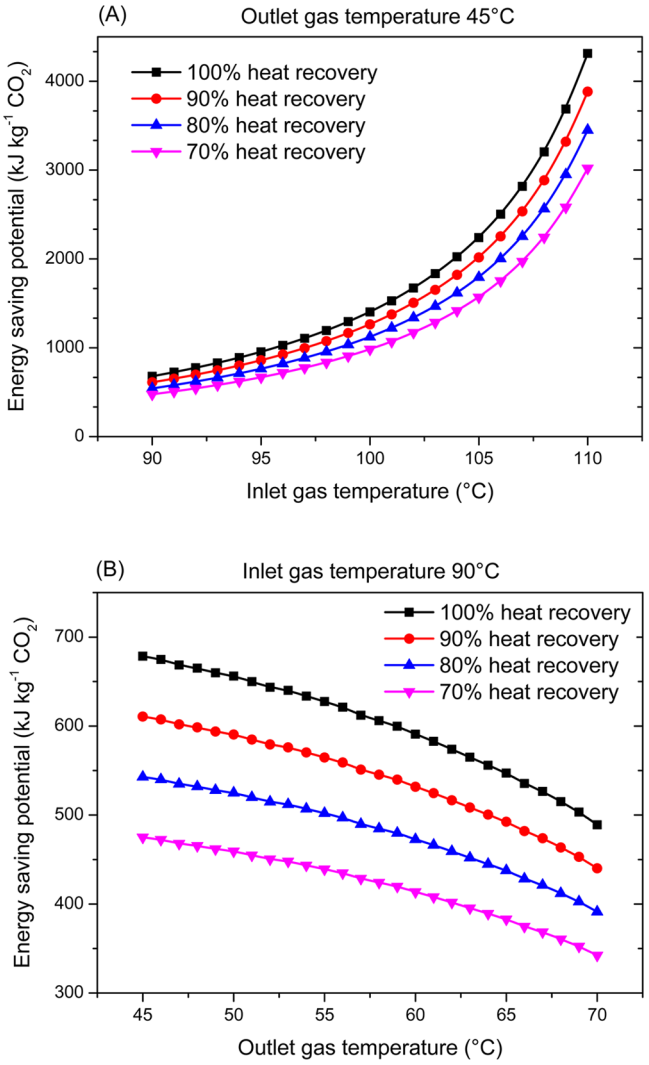

Figure 2. Energy-saving potential with variation of (A) inlet gas temperature (constant outlet temperature = 45 °C), and (B) outlet gas temperature (constant inlet temperature = 90 °C). Estimation is based on the Tarong postcombustion carbon capture pilot plant with a carbon capture capacity of 70 kg·h^{-1} (data shown in Table 1).

membrane module, respectively. $J_m(x)$ is the transmembrane vapor flux (kilograms per square meter per hour), which is a function of the driving force and membrane permeability.

The driving force of mass transfer in this process is the partial vapor pressure difference across the membrane; hence, the vapor flux across the membrane can expressed as

$$J_m(x) = K[P_h(x) - P_c(x)] = K\Delta P(x) \tag{11}$$

where K is the overall (empirical) mass-transfer coefficient (kilograms per square meter per hour per pascal) and $\Delta P(x)$ is the bulk partial vapor pressure difference between hot feed stream and cold permeate stream at position x. Note that K accounts for permeability of the membrane as well as the boundary layer effect, which is relevant to the flow hydrodynamics.

2.3.2. Heat Transfer across Membrane Condenser. Heat transfer across the membrane condenser involves convective heat transfer via water vapor flow and conductive heat transfer through the membrane material. The heat flux (q_m) at some location within the membrane (in direction z) is given by[36,37]

$$q_m = J_m h_v[T(z)] - \lambda_m \frac{dT(z)}{dz} \tag{12}$$

where $h_v(T)$ is the vapor enthalpy at temperature T.

The water vapor enthalpy as a function of temperature can be described by

$$h_v(T) = h_v(T_0) + \int_{T_0}^{T} c_{p,v}\, dT \tag{13}$$

where $h_v(T_0)$ is the water vapor enthalpy at reference temperature T_0 and $c_{p,v}$ is the specific heat of water vapor. When the temperature change across the membrane is in the range of a few degrees, $c_{p,v}$ can be assumed to be constant, and thus eq 13 can be derived into

$$h_v(T) = h_v(T_0) + c_{p,v}(T - T_0) \tag{14}$$

After substitution of eq 14 into eq 12, the following can be obtained:

$$\int_{T_h}^{T_c} \frac{1}{J_m c_{p,v} T + J_m[h_v(T_0) - c_{p,v}T_0] - Q_m} dT = \frac{1}{\lambda_m}\int_0^{\delta_m} dz \tag{15}$$

Then, we can obtain

$$Q_m = J_m\left[h_v(T_0) - c_{p,v}T_0 + \frac{c_{p,v}[T_h \exp(BJ_m) - T_c]}{\exp(BJ_m) - 1}\right] \tag{16}$$

where B is a constant, defined as

$$B = \frac{c_{p,v}\delta_m}{\lambda_m} \tag{17}$$

Based on eqs 12 and 16, the conductive heat transfer at the cold liquid-membrane interface (η_c) can be expressed as

$$\eta_c = -\lambda_m \frac{dT}{dz}\bigg|_{T=T_c} = Q_m - J_m H_v(T_c) = \frac{J_m c_{p,v}\exp(BJ_m)}{\exp(BJ_m) - 1}(T_h - T_c) \tag{18}$$

Similarly, the conductive heat transfer at the hot gas-membrane interface (η_h) can be expressed as

$$\eta_h = -\lambda_m \frac{dT}{dz}\bigg|_{T=T_h} = Q_m - J_m H_v(T_h) = \frac{J_m c_{p,v}}{\exp(BJ_m) - 1}(T_h - T_c) \tag{19}$$

The difference between conductive heat transfer at the cold liquid−membrane interface and at the hot gas−membrane interface can be written as

$$\Delta\eta = -\lambda_m \frac{dT}{dz}\bigg|_{T=T_c} + \lambda_m \frac{dT}{dz}\bigg|_{T=T_h} = J_m c_{p,v}(T_h - T_c) \tag{20}$$

which is actually the difference between the enthalpy of water vapor at T_h and that at T_c.

2.3.3. Heat Transfer along Membrane Condenser. The heat flux reaching the cold liquid stream consists of (i) enthalpy

DOI: 10.1021/es504526s
Environ. Sci. Technol. 2015, 49, 2532−2540

of condensation at T_c, (ii) inherent enthalpy of condensed water, and (iii) conductive heat transfer (η_c). Therefore, the total enthalpy change of cold liquid in a differential segment of the membrane channel can be written as[38]

$$\frac{\mathrm{d}[m_c(x)h_w(T_c)]}{\mathrm{d}x} = \frac{\mathrm{d}m_c(x)}{\mathrm{d}x}[h_{vap}(T_c) + h_w(T_c)] + \frac{A}{L}\eta_c(x) \tag{21}$$

where h_{vap} and h_w are the specific enthalpies of vaporization and water, respectively.

Similarly, heat flux at the hot gas−membrane interface can be expressed as

$$\frac{\mathrm{d}[m_c(x)h_w(T_h)]}{\mathrm{d}x} = \frac{\mathrm{d}m_h(x)}{\mathrm{d}x}[h_{vap}(T_h) + h_w(T_h)] + \frac{A}{L}\eta_h(x) \tag{22}$$

In this scenario, the heat balance can be expressed as

$$Q_c = Q_r \tag{23}$$

namely,

$$m_1 c_{p,c}(T_{c,o} - T_{c,i}) + m_{10}h_w(T_{c,o}) = m_{7,H_2O}h_{7,H_2O} - m_{6,H_2O}h_{6,H_2O} + (h_{7,H_2O} - h_{6,H_2O})m_{CO_2} \tag{24}$$

where $h_w(T_{c,o})$ is the specific enthalpy of liquid water at the outlet solvent stream temperature ($T_{c,o}$).

2.4. Scenario 3: Partial Mass Transfer through Membrane into Absorbent. In this scenario, partial water vapor in the gas stream (S_6) transfers across the membrane and then condenses into the cold absorbent, and the remaining vapor condenses at the membrane surface on the hot gas side. We introduce a new parameter, γ, called the mass-transfer ratio. This scenario is most likely to happen in practical applications. The mass balance (see Figure 1) then can be written as

$$m_8 + m_{10} = m_6 - m_7 \tag{25}$$

where

$$m_{10} = \gamma(m_6 - m_7) \tag{26}$$

and

$$m_8 = (1 - \gamma)(m_6 - m_7) \tag{27}$$

When $\gamma = 0$, this is scenario 1. When $\gamma = 1$, this is scenario 2.

2.4.1. Mass Transfer across Membrane Condenser. Mass transfer across the membrane is similar to that in scenario 2; refer to eqs 10 and 11. Vapor condensation at the hot gas−membrane interface has two effects: reducing the vapor quantity in the hot gas stream and increasing the gas stream temperature due to the released latent heat via condensation. The former effect could lower the vapor partial pressure, while the latter could increase the vapor partial pressure. Therefore, the vapor flux in scenario 3 can be higher or lower than that in scenario 2, depending on which effect is dominant.

2.4.2. Heat Transfer across Membrane Condenser. The heat obtained on the cold absorbent side (Q_c) can be expressed as

$$Q_c = m_9 h_{c,o} - m_1 h_{c,i} = m_1 c_{p,c}(T_{c,o} - T_{c,i}) + m_{10}h_w(T_{c,o}) \tag{28}$$

The heat back to the desorber on the hot gas side (Q_8) and the total heat recovery (Q_r) are given by eqs 5 and 6. Therefore, the heat balance can be written as

$$Q_c + Q_8 = Q_r \tag{29}$$

namely,

$$m_1 c_{p,c}(T_{c,o} - T_{c,i}) + m_{10}h_w(T_{c,o}) + m_8 h_w(T_{h,i}) = m_{7,H_2O}h_{7,H_2O} - m_{6,H_2O}h_{6,H_2O} + (h_{7,CO_2} - h_{6,CO_2})m_{CO_2} \tag{30}$$

According to eqs 1 and 16, the heat transferred across the membrane in scenario 3 is a combination of conductive heat and convective heat, which can be written as

$$Q_m = H_m A(T_h - T_c) + J_m\left[h_v(T_0) - c_{p,v}T_0 + \frac{c_{p,v}[T_h \exp(BJ_m) - T_c]}{\exp(BJ_m) - 1}\right] \tag{31}$$

Here

$$Q_c = Q_m = Q_r - Q_8 \tag{32}$$

2.5. Overall Heat-Transfer Coefficient. Heat transfer across the membrane in the condensation system can be very complicated because it may involve heat transfer across the boundary layer and condensed liquid film[39] and with noncondensable gas (e.g., CO_2).[40] To simplify the situation, we use the overall heat-transfer coefficient (U in watts per square meter per kelvin), which accounts for membrane resistance and all other external factors (e.g., boundary layer effect and condensate film). Total heat transfer across the membrane (Q_m) is given by

$$Q_m = UA\Delta T \tag{33}$$

with

$$\Delta T = \frac{(T_{h,in} - T_{c,out}) - (T_{h,out} - T_{c,in})}{\ln\left(\frac{T_{h,in} - T_{c,out}}{T_{h,out} - T_{c,in}}\right)} \tag{34}$$

ΔT is a log mean temperature difference (kelvins), commonly used in countercurrent heat exchange.

2.6. Energy Saving in Reboiler Duty. When a standard stripper without rich split is taken as the reference case and the reboiler, stripper, and lean/rich heat exchanger are considered as a unit, the reboiler duty (Q_R, kilojoules per kilogram of CO_2) can be evaluated according to the overall heat balance:

$$Q_R = \Delta h_{CO_2} + h_G(t_6)m_6 + h_L(t_5)m_5 - h_L(t_2)m_2 \tag{35}$$

where Δh_{CO_2} is the enthalpy for CO_2 desorption, h_G is the enthalpy of the gas stream over the stripper, and h_L is the enthalpy of the liquid solvent.

Similarly, when rich split is adopted, the reboiler duty can be expressed as

$$Q_R = \Delta h_{CO_2} + h_G(t_7)m_7 + h_L(t_5)m_5 - h_L(t_1)m_1 - h_L(t_2)m_2 \tag{36}$$

Ideally, when the cold lean solvent temperature (t_5), regeneration temperature (t_4), and heat-transfer efficiency of the lean/rich heat exchanger are fixed, the energy-saving potential in the reboiler duty (ΔQ_R, kilojoules per kilogram of CO_2) via membrane condenser compared with the reference case can be estimated by

DOI: 10.1021/es504526s
Environ. Sci. Technol. 2015, 49, 2532−2540

$$\Delta Q_R = h_G(t_6^B)m_6^B - h_G(t_7)m_7 \quad (37)$$

Obviously, ΔQ_R is determined by the properties of the gas stream over the stripper in the reference case (t_6^B, m_6^B) and those of the gas stream after heat recovery by the membrane condenser (t_7, m_7).

3. RESULTS AND DISCUSSION

3.1. Rich Split Modification. As shown in Figure 1, the CO_2-rich solvent is split after absorption into two streams (S_1 and S_2). This process modification, called rich split, can reduce both reboiler and condenser duty in conventional carbon capture processes.[14,15] However, there is a minimum flow rate for S_2 to maintain $t_4 > t_3$. The relationship between t_3 and the split mass flow rates (m_1 and m_2) is shown in Figure S2 in Supporting Information. It is calculated that the split mass flow m_1 is in the range 0−742 kg·h^{-1} (0−37%) and m_2 is in the range 1258−2000 kg·h^{-1} (63−100%), according to the data from our Tarong pilot plant.

3.2. Heat Recovery with Membrane Condenser. The gas stream (containing CO_2 and water vapor) released from the desorber (S_6) is water-saturated at high temperatures. The temperature of this stream (t_6) is around 90 °C after cooling by reflux from the traditional condenser. If a membrane condenser is integrated into the process, t_6 can be higher, because the reflux is lower than that in a traditional condenser. In practical operations, the inlet gas temperature (t_6) may also vary with the type of absorbent selected. Figure 2 shows the energy-saving potential of the membrane condenser with variation of the inlet and outlet gas temperatures (compared with the situation without heat recovery by rich split, as shown in Figure S1 in Supporting Information). Heat recovery increases exponentially with rising inlet gas temperature (t_6). However, higher inlet gas temperature also means higher reboiler duty caused by the higher water vapor pressure and thus more latent heat, which is undesirable in the process. For a given absorbent, t_6 is relatively stable, and the reasonable way to achieve energy savings is to minimize the outlet gas temperature by employing membranes with large heat-transfer coefficients.

It is also obvious that heat recovery is reduced significantly as outlet gas temperature (t_7) increases. Therefore, outlet gas temperature needs to be reduced in practical operations. According to eq 33, selecting membranes with high heat-transfer coefficients and maintaining large contact areas can improve heat transfer across the membrane and thus effectively reduce the outlet gas temperature. If the outlet gas temperature is low enough, it may be unnecessary to have a traditional condenser after the desorber, thereby saving a considerable amount of cooling water. Note that to maintain mass and/or heat transfer, the outlet gas temperature (t_7) is always higher than the inlet liquid temperature (t_1).

Compared to conventional condensers in the standard rich split process,[14,20] a membrane condenser may help achieve lower reboiler duty. Cousins et al.[14] reported that when ∼30% cold rich solvent is bypassed to a conventional condenser, temperature of the gas stream from the stripper is 90−95 °C and the reboiler duty reduction is around 400 kJ·(kg of CO_2)$^{-1}$ compared with the standard PCC process without rich split. In this study, energy savings (i.e., reboiler duty reduction) can vary from 500 to 650 kJ·(kg of CO_2) when the inlet gas temperature is 90 °C and there is no heat loss in the membrane condenser (i.e., 100% heat recovery), as shown in Figure 2B.

Typical heat-transfer coefficients of different membranes are summarized in Table S1 (Supporting Information). They are generally in the order porous polymeric membranes < dense polymeric membranes (or high-porosity < low-porosity polymeric membranes) < wetted porous membranes < dense metal membranes. It must be noted that these heat-transfer coefficients are based on thermal conductive heat transfer only; for porous membranes, convective heat transfer associated with mass transfer could be much larger than conductive heat transfer. Therefore, the total heat-transfer coefficients of porous polymeric membranes are expected to be larger than those of wetted porous and/or dense polymeric membranes where convective heat transfer is restricted.

In the membrane condensation application, the overall heat-transfer coefficient (U) can be much lower than the heat-transfer coefficient of the membrane itself. This is because of the extra heat-transfer resistance, caused by factors such as the boundary layer and the condensate film.[39] Typical values of the overall heat-transfer coefficient for a heat exchanger are generally in the range of $(2 \times 10^2)-(2 \times 10^3)$ W·m^{-2}·K^{-1}.[41] In the following analysis, we choose different overall heat-transfer coefficients (U = 250, 500, 1000, and 2000 W·m^{-2}·K^{-1}) for comparison.

3.3. Scenario 1: Limited Mass Transfer across Membrane. In scenario 1, there is no mass transfer across the membrane and most of the water vapor in the hot gas stream condenses on the membrane surface and goes back to the desorber. When a porous membrane becomes wetted or a dense membrane is used in the condensation system, scenario 1 fits the situation, and the membrane condenser can be regarded as a conventional heat exchanger. The condensate flow rate (m_8) is dependent on the outlet gas temperature. As outlet gas temperature rises, the condensate flow rate is reduced, but the water vapor content in the outlet gas stream increases significantly (Figure S3, Supporting Information).

Figure 3 shows the required membrane area and outlet rich solvent temperature with variation of split mass flow rate m_1 in this scenario. When the inlet gas stream temperature is 90 °C (Figure 3A), the minimum value of the split mass flow rate (m_1) is about 250 kg·h^{-1}. As m_1 increases from 250 to 300 kg·h^{-1}, the required membrane area is reduced dramatically. At the same time, the outlet solvent temperature is reduced from 90 to 84 °C. In practical operations, it is desirable to use less membrane area and maintain a reasonable temperature difference (e.g., 10−15 °C) across the membrane. It is estimated that the optimal split mass flow rates of m_1 are 340−400 kg·h^{-1}.

When the inlet gas stream temperature is 100 °C, the minimum value of the split mass flow rate (m_1) increases to ∼450 kg·h^{-1} (Figure 3B). As m_1 increases from 450 to 500 kg·h^{-1}, the required membrane area is reduced dramatically and the outlet solvent temperature is reduced almost linearly, from 100 to 94 °C. Similarly, the estimated optimal split mass flow rates of m_1 are 530−600 kg·h^{-1}. The required membrane area is strongly dependent on the overall heat-transfer coefficient as shown in Figure 3 and eq 33, particularly when t_6 is higher.

3.4. Scenario 2: Complete Mass Transfer through Membrane. In this scenario, there is no water vapor condensation on the gas side and all water vapor in the gas stream (S_6) transfers and then condenses into the cold solvent. This means that heat recovery is completely realized by heating the cold solvent. Under the same conditions, therefore, the required membrane area should be larger than that in scenario

DOI: 10.1021/es504526s
Environ. Sci. Technol. 2015, 49, 2532−2540

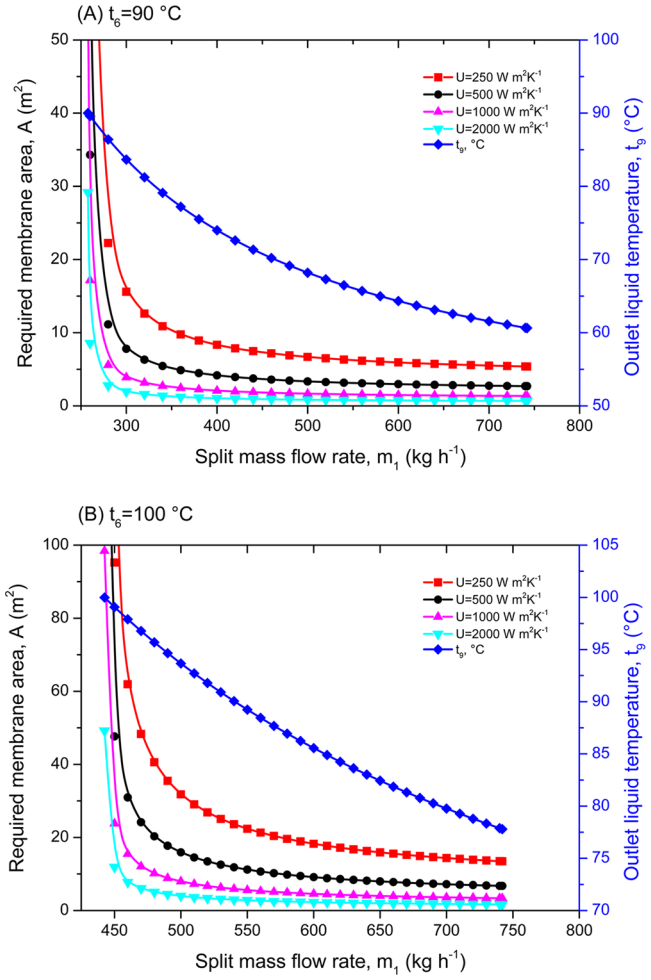

Figure 3. Estimated membrane area and outlet liquid temperature with variation of split mass flow rate m_1 in scenario 1: temperature of the gas stream from the stripper (t_6) is (A) 90 or (B) 100 °C. Estimation is based on the Tarong postcombustion carbon capture pilot plant with a carbon capture capacity of 70 kg·h^{-1} (see Table 1).

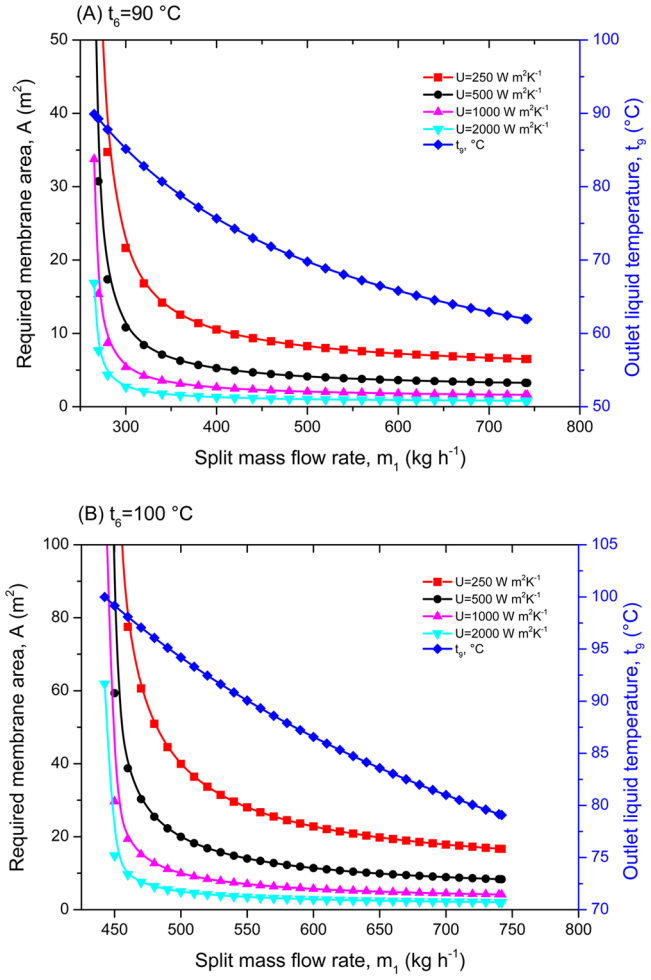

Figure 4. Estimated membrane area and outlet liquid temperature with variation of split mass flow rate m_1 in scenario 2: temperature of the gas stream from the stripper (t_6) is (A) 90 or (B) 100 °C. Estimation is based on the Tarong postcombustion carbon capture pilot plant with a carbon caputre capacity of 70 kg·h^{-1} (see Table 1).

1, and the outlet solvent temperature is higher. Figure 4 presents the estimated membrane area and outlet liquid temperature with variation of the split mass flow rate (m_1) in scenario 2. As expected, the required membrane area is larger and outlet solvent temperature is higher under the same conditions in scenario 2. For example, when U = 500 W·m^{-2}·K^{-1}, t_6 = 90 °C, and m_1 = 300 kg·h^{-1}, the required membrane areas are 8 m^2 in scenario 1 and 10 m^2 in scenario 2, while the outlet solvent temperatures are 83 °C in scenario 1 and 85 °C in scenario 2.

Correspondingly, the optimal split mass flow rate for scenario 2 should be slightly larger than that in scenario 1. It is estimated that, in scenario 2, the optimal split mass flow rates m_1 at t_6 = 90 °C are 360−420 kg·h^{-1} and at t_6 = 100 °C are 550−620 kg·h^{-1}.

3.5. Scenario 3: Partial Mass Transfer through Membrane. In this scenario, partial water vapor in the gas stream (S_6) transfers across the membrane and then condenses into cold absorbent; the remaining water vapor condenses at the membrane surface and goes back to desorber on the hot gas side. Heat recovery is realized by heating the cold solvent and the condensate (i.e., liquid water) with some heat on both sides of the membrane flowing back to the desorber.

Figure 5 describes the effect of mass-transfer ratio (γ) on membrane area and outlet solvent temperature. It can be seen that both the required membrane area and the outlet solvent temperature slightly increase as the mass-transfer ratio increases from 0 to 100%. This suggests that mass transfer does not significantly affect heat recovery in the membrane condensation system. Therefore, although membrane wetting is a challenge in traditional applications of membrane contactors,[42] it may not be a severe issue in membrane condensation applications.

Looking carefully, we find that with different mass-transfer ratios the change in membrane area becomes less obvious. However, the change in outlet solvent temperature becomes more obvious as the split mass flow rate (m_1) increases. Comparing Figure 5 panels A and B, we also find that both the minimum split mass flow rate (m_1) and minimum outlet solvent temperature are higher at higher inlet gas temperatures (t_6).

The preceding analysis outlines a general picture of the energy-saving potential of a membrane condenser, compared with the reference condition without any heat recovery via rich split, and explores the effects of some variables such as mass transfer and split mass flow rates on process performance. Heat recovery performance is mainly dependent on membrane properties, such as thickness, pore size, porosity, and thermal

DOI: 10.1021/es504526s
Environ. Sci. Technol. 2015, 49, 2532−2540

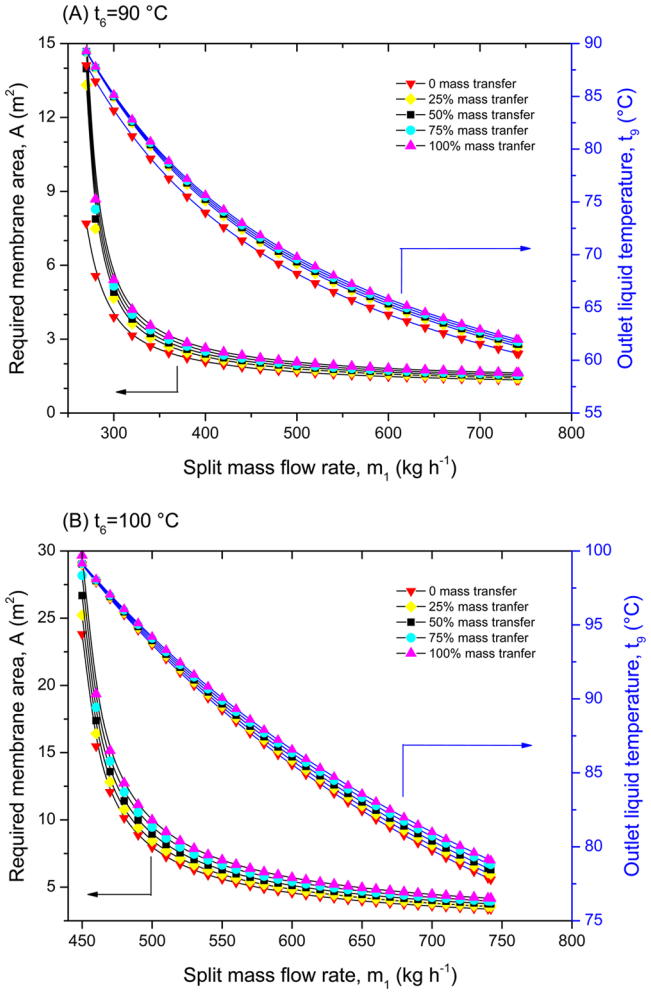

Figure 5. Estimated membrane area and outlet liquid temperature with variation of split mass flow rate m_1 in scenario 3: temperature of the gas stream from the stripper (t_6) is (A) 90 or (B) 100 °C. The overall heat-transfer coefficient U = 1000 $W{\cdot}m^{-2}{\cdot}K^{-1}$. Estimation is based on the Tarong postcombustion carbon capture pilot plant with a carbon capture capacity of 70 $kg{\cdot}h^{-1}$ (see Table 1).

conductivity. Since these properties vary between membranes, it is difficult to compare the energy-saving performance or costs of membrane condensers and traditional condensers. However, our study provides important insights into energy recovery performance and the selection of parameters such as split mass flow rates and membrane properties. Future research should evaluate energy-saving performance by comparing specific membranes with known properties to traditional condensers.

In the membrane condensation system, heat recovery increases significantly with rising inlet gas temperature and decreasing outlet gas temperature. To achieve minimum membrane area and reasonable temperature difference (i.e., driving force) across the membrane, there is an optimal split mass flow rate that is determined by the inlet gas temperature and the overall heat-transfer coefficient in the condensation system. Our analysis provides important insights into energy recovery performance and the selection of operational parameters, such as split mass flow rate and membrane thickness, area, and thermal conductivity, in the membrane condensation system.

■ ASSOCIATED CONTENT

Supporting Information

Three figures showing typical liquid-absorbent-based post-combustion carbon capture process, relationship between t_3 and split mass flow rates, and effect of outlet gas temperature on condensate flow rate and water vapor flow rate in scenario 1; one table listing typical thermal conductivities and heat-transfer coefficients of different membranes based on eq 2. This material is available free of charge via the Internet at http://pubs.acs.org/.

■ AUTHOR INFORMATION

Corresponding Author

*E-mail shuaifei.zhao@csiro.au; tel +61 2 49606127.

Notes

The authors declare no competing financial interest.

■ ACKNOWLEDGMENTS

This work was carried out within CSIRO's Energy Flagship. We thank Dr. Ashleigh Cousins for providing the data on operating the Tarong PCC pilot plant. Special thanks also go to Drs. Ashleigh Cousins, Shihong Lin, Eric Favre, Zongli Xie, and Daniel Roberts for their helpful comments in the preparation of this paper.

■ REFERENCES

(1) Merkel, T. C.; Lin, H.; Wei, X.; Baker, R. Power plant post-combustion carbon dioxide capture: An opportunity for membranes. *J. Membr. Sci.* **2010**, *359* (1−2), 126−139.

(2) Wang, M.; Lawal, A.; Stephenson, P.; Sidders, J.; Ramshaw, C. Post-combustion CO_2 capture with chemical absorption: A state-of-the-art review. *Chem. Eng. Res. Des.* **2011**, *89* (9), 1609−1624.

(3) Luis, P.; Van Gerven, T.; Van der Bruggen, B. Recent developments in membrane-based technologies for CO_2 capture. *Prog. Energy Combust. Sci.* **2012**, *38* (3), 419−448.

(4) Davison, J. Performance and costs of power plants with capture and storage of CO_2. *Energy* **2007**, *32* (7), 1163−1176.

(5) Bara, J. E. What chemicals will we need to capture CO_2? *Greenhouse Gases: Sci. Technol.* **2012**, *2* (3), 162−171.

(6) Yong, Z.; Mata, V.; Rodrigues, A. r. E. Adsorption of carbon dioxide at high temperature: A review. *Sep. Purif. Technol.* **2002**, *26* (2−3), 195−205.

(7) Kim, S.; Lee, Y. M. High performance polymer membranes for CO_2 separation. *Curr. Opin. Chem. Eng.* **2013**, *2* (2), 238−244.

(8) Luis, P.; Van der Bruggen, B. The role of membranes in post-combustion CO_2 capture. *Greenhouse Gases: Sci. Technol.* **2013**, *3* (5), 318−337.

(9) Brunetti, A.; Scura, F.; Barbieri, G.; Drioli, E. Membrane technologies for CO_2 separation. *J. Membr. Sci.* **2010**, *359* (1−2), 115−125.

(10) Figueroa, J. D.; Fout, T.; Plasynski, S.; McIlvried, H.; Srivastava, R. D. Advances in CO_2 capture technology: The U.S. Department of Energy's carbon sequestration program. *Int. J. Greenhouse Gas Control* **2008**, *2* (1), 9−20.

(11) Feron, P. H. M. Exploring the potential for improvement of the energy performance of coal fired power plants with post-combustion capture of carbon dioxide. *Int. J. Greenhouse Gas Control* **2010**, *4* (2), 152−160.

(12) Cottrell, A. J.; McGregor, J. M.; Jansen, J.; Artanto, Y.; Dave, N.; Morgan, S.; Pearson, P.; Attalla, M. I.; Wardhaugh, L.; Yu, H.; Allport, A.; Feron, P. H. M. Post-combustion capture R & D and pilot plant operation in Australia. *Energy Proc.* **2009**, *1* (1), 1003−1010.

(13) Feron, P. H. M. The potential for improvement of the energy performance of pulverized coal fired power stations with post-combustion capture of carbon dioxide. *Energy Proc.* **2009**, *1* (1), 1067−1074.

DOI: 10.1021/es504526s
Environ. Sci. Technol. 2015, 49, 2532−2540

(14) Cousins, A.; Wardhaugh, L. T.; Feron, P. H. M. Preliminary analysis of process flow sheet modifications for energy efficient CO_2 capture from flue gases using chemical absorption. *Chem. Eng. Res. Des.* **2011**, *89* (8), 1237−1251.
(15) Cousins, A.; Wardhaugh, L. T.; Feron, P. H. M. A survey of process flow sheet modifications for energy efficient CO_2 capture from flue gases using chemical absorption. *Int. J. Greenhouse Gas Control* **2011**, *5* (4), 605−619.
(16) Cousins, A.; Wardhaugh, L. T.; Feron, P. H. M. Analysis of combined process flow sheet modifications for energy efficient CO_2 capture from flue gases using chemical absorption. *Energy Proc.* **2011**, *4*, 1331−1338.
(17) Puxty, G.; Rowland, R.; Allport, A.; Yang, Q.; Bown, M.; Burns, R.; Maeder, M.; Attalla, M. Carbon dioxide postcombustion capture: A novel screening study of the carbon dioxide absorption performance of 76 amines. *Environ. Sci. Technol.* **2009**, *43* (16), 6427−6433.
(18) Artanto, Y.; Jansen, J.; Pearson, P.; Puxty, G.; Cottrell, A.; Meuleman, E.; Feron, P. Pilot-scale evaluation of AMP/PZ to capture CO_2 from flue gas of an Australian brown coal-fired power station. *Int. J. Greenhouse Gas Control* **2014**, *20*, 189−195.
(19) Cousin, A.; Cottrell, A.; Huang, S.; Feron, P. H. M.; Lawson, A. Tarong CO_2 capture pilot plant. *Energy Gener.* **2012**, 16−17.
(20) Lin, Y.-J.; Madan, T.; Rochelle, G. T. Regeneration with rich bypass of aqueous piperazine and monoethanolamine for CO_2 capture. *Ind. Eng. Chem. Res.* **2014**, *53* (10), 4067−4074.
(21) Zhao, S.; Cao, C.; Wardhaugh, L.; Feron, P. H. M. Membrane evaporation of amine solution for energy saving in post-combustion carbon capture: Performance evaluation. *J. Membr. Sci.* **2015**, *473*, 274−282.
(22) Feron, P. H. M.; Zhao, S. *Membrane Assisted Liquid Absorbent Regeneration (MALAR): Innovative Use of Membranes in Liquid Absorbent Based CO_2 Capture*, 2013 AIChE Annual Meeting, San Francisco, CA, 2013.
(23) Zhang, Y.; Wang, R. Novel method for incorporating hydrophobic silica nanoparticles on polyetherimide hollow fiber membranes for CO_2 absorption in a gas−liquid membrane contactor. *J. Membr. Sci.* **2014**, *452*, 379−389.
(24) Scholes, C. A.; Qader, A.; Stevens, G. W.; Kentish, S. E. Membrane gas-solvent contactor pilot plant trials of CO_2 absorption from flue gas. *Sep. Sci. Technol.* **2014**, *49* (16), 2449−2458.
(25) Wang, Z.; Fang, M.; Yu, H.; Wei, C.-C.; Luo, Z. Experimental and modeling study of trace CO_2 Removal in a hollow-fiber membrane contactor, using CO_2-loaded monoethanolamine. *Ind. Eng. Chem. Res.* **2013**, *52* (50), 18059−18070.
(26) Gabelman, A.; Hwang, S.-T. Hollow fiber membrane contactors. *J. Membr. Sci.* **1999**, *159* (1−2), 61−106.
(27) Yan, S.; He, Q.; Zhao, S.; Wang, Y.; Ai, P. Biogas upgrading by CO_2 removal with a highly selective natural amino acid salt in gas-liquid membrane contactor. *Chem. Eng. Process.: Process Intensif.* **2014**, *85*, 125−135.
(28) Chabanon, E.; Belaissaoui, B.; Favre, E. Gas−liquid separation processes based on physical solvents: opportunities for membranes. *J. Membr. Sci.* **2014**, *459*, 52−61.
(29) Zhang, Y.; Wang, R. Gas-liquid membrane contactors for acid gas removal: Recent advances and future challenges. *Curr. Opin. Chem. Eng.* **2013**, *2* (2), 255−262.
(30) Cousins, A.; Cottrell, A.; Lawson, A.; Huang, S.; Feron, P. H. M. Model verification and evaluation of the rich-split process modification at an Australian-based post combustion CO_2 capture pilot plant. *Greenhouse Gases: Sci. Technol.* **2012**, *2* (5), 329−345.
(31) Weiland, R. H.; Dingman, J. C.; Cronin, D. B. Heat capacity of aqueous monoethanolamine, diethanolamine, *N*-methyldiethanol-amine, and *N*-methyldiethanolamine-based blends with carbon dioxide. *J. Chem. Eng. Data* **1997**, *42* (5), 1004−1006.
(32) Chiu, L.-F.; Liu, H.-F.; Li, M.-H. Heat capacity of alkanolamines by differential scanning calorimetry. *J. Chem. Eng. Data* **1999**, *44* (3), 631−636.
(33) Agbonghae, E. O.; Hughes, K. J.; Ingham, D. B.; Ma, L.; Pourkashanian, M. A semi-empirical model for estimating the heat capacity of aqueous solutions of alkanolamines for CO_2 capture. *Ind. Eng. Chem. Res.* **2014**, *53* (19), 8291−8301.
(34) Schofield, R. W.; Fane, A. G.; Fell, C. J. D. Heat and mass transfer in membrane distillation. *J. Membr. Sci.* **1987**, *33* (3), 299−313.
(35) Lawson, K. W.; Lloyd, D. R. Membrane distillation. *J. Membr. Sci.* **1997**, *124* (1), 1−25.
(36) Gryta, M.; Tomaszewska, M. Heat transport in the membrane distillation process. *J. Membr. Sci.* **1998**, *144* (1−2), 211−222.
(37) Phattaranawik, J.; Jiraratananon, R. Direct contact membrane distillation: Effect of mass transfer on heat transfer. *J. Membr. Sci.* **2001**, *188* (1), 137−143.
(38) Lin, S.; Yip, N. Y.; Elimelech, M. Direct contact membrane distillation with heat recovery: Thermodynamic insights from module scale modeling. *J. Membr. Sci.* **2014**, *453*, 498−515.
(39) Jeong, K.; Kessen, M. J.; Bilirgen, H.; Levy, E. K. Analytical modeling of water condensation in condensing heat exchanger. *Int. J. Heat Mass Transfer* **2010**, *53* (11−12), 2361−2368.
(40) Karkoszka, K. *Mechanistic modelling of water vapour condensation in presence of noncondensable gases*. Ph.D. Thesis, KTH Royal Institute of Technology, Stockholm, Sweden, 2007.
(41) Incropera, F. P.; DeWitt, D. P. *Fundamentals of Heat and Mass Transfer*, 2nd ed.; John Wiley & Sons: New York, 1985.
(42) Mosadegh-Sedghi, S.; Rodrigue, D.; Brisson, J.; Iliuta, M. C. Wetting phenomenon in membrane contactors: Causes and prevention. *J. Membr. Sci.* **2014**, *452*, 332−353.

DOI: 10.1021/es504526s
Environ. Sci. Technol. 2015, 49, 2532−2540